Available online at www.sciencedirect.com

ScienceDirect

Biomedical Journal

journal homepage: www.elsevier.com/locate/bj

Review Article

The binding and specificity of chemokine binding proteins, through the lens of experiment and computation

Lauren E. Stark [a,1], *Wenyan Guan* [b,1], *Michael E. Colvin* [a,c], *Patricia J. LiWang* [a,b,d,*]

[a] *Quantitative and Systems Biology Graduate Group, University of California, USA*
[b] *Materials and Biomaterials Science and Engineering, University of California, USA*
[c] *Department of Chemistry and Biochemistry, University of California, USA*
[d] *Department of Molecular and Cell Biology, University of California, USA*


Prof. Patricia J. LiWang

ARTICLE INFO

Article history:
Received 9 May 2021
Accepted 19 July 2021
Available online 24 July 2021

Keywords:
viral CC Chemokine Inhibitor (vCCI)
35K
Chemokine inhibitor
Chemokine binding protein
Chemokine
Molecular dynamics

ABSTRACT

Chemokines are small proteins that are critical for immune function, being primarily responsible for the activation and chemotaxis of leukocytes. As such, many viruses, as well as parasitic arthropods, have evolved systems to counteract chemokine function in order to maintain virulence, such as binding chemokines, mimicking chemokines, or producing analogs of transmembrane chemokine receptors that strongly bind their targets. The focus of this review is the large group of chemokine binding proteins (CBP) with an emphasis on those produced by mammalian viruses. Because many chemokines mediate inflammation, these CBP could possibly be used pharmaceutically as anti-inflammatory agents. In this review, we summarize the structural properties of a diverse set of CBP and describe in detail the chemokine binding properties of the poxvirus-encoded CBP called vCCI (viral CC Chemokine Inhibitor). Finally, we describe the current and emerging capabilities of combining computational simulation, structural analysis, and biochemical/biophysical experimentation to understand, and possibly re-engineer, protein–protein interactions.

This is an exciting time in molecular immunology. Increasing capabilities in areas like structural biology and molecular simulation are providing powerful new scientific tools for deciphering the immune system. At the same time, there is a critical need for new therapies against emerging infectious diseases, such as that caused by the virus SARS-CoV-2, and other diseases associated with a dysregulated immune response. This review describes current results and future directions in the study of the molecular function of the soluble chemokine binding proteins (CBP, sometimes called CKBP),

* *Corresponding author*. Quantitative and Systems Biology Graduate Group, University of California, 5200 N. Lake Rd., Merced, CA 95343, USA.
E-mail address: pliwang@ucmerced.edu (P.J. LiWang).
Peer review under responsibility of Chang Gung University.
[1] These two authors contributed equally to this work.
https://doi.org/10.1016/j.bj.2021.07.004

with a focus on the poxvirus-encoded protein viral CC Chemokine Inhibitor (vCCI). As described below, these proteins are one component in the strategy used by mammalian viruses and various organisms to suppress their host's immune response. These proteins have the interesting property that they bind with high specificity to entire classes of immune-signaling chemokines. Elucidating how these proteins specifically recognize their various chemokine ligands could allow the re-engineering of CBP for use as therapeutics.

This review begins by giving a brief background on chemokines and the different tools that viruses use to reduce the infected host's chemokine effectiveness. Then we describe the structural features of a range of CBP that provide hints to the common structural elements that mediate chemokine binding. This section includes a tabular summary of the properties of these proteins and figures highlighting their key features.

After that summary, we describe in detail the chemokine-binding properties of rabbitpox protein vCCI as an archetype of the viral CBP. We also describe how molecular simulations, structural analysis, mutation studies, and biochemical/biophysical assays can be combined to elucidate a detailed map of how the structural features of vCCI determine its chemokine binding specificity. Finally, we end with a look forward to how this structural information can be used to reengineer CBP or chemokines for specific biomedical or biotechnological applications.

Background

The immune system serves a variety of functions in protecting human health, and a critical aspect of the immune response is the activation and chemotaxis of immune cells, as mediated by chemokines. When injury or infection occurs, chemokines are secreted, producing an inflammatory immune response. Chemokines are small proteins (usually about 70 amino acids) that tightly bind their cognate 7-transmembrane receptor and are also able to bind glycosaminoglycans (GAGs). Their mode of action is generally to first bind GAGs on the endothelial surface, setting up a chemokine concentration gradient. They then bind tightly to their respective receptors on the surface of passing leukocytes, which are activated by this binding event. Chemokine-receptor interactions, including those involved in non-inflammatory processes, have been recently reviewed [1, 2].

There are four subfamilies of chemokines, totaling about 50 members, named based on the placement of conserved cysteines near the N-terminus of the protein (CC, CXC, CX3C, and C), with chemokines from all subfamilies having the same overall fold. The name of each chemokine is based on its subfamily type, followed by L (to signify it is a ligand of a chemokine receptor), followed by a number to distinguish different specific molecules, e.g. CCL4. For a table correlating older chemokine names with this numerical naming system, see Supplemental Table 1. The different subfamilies exert their influence on different receptors affecting different leukocyte populations [2]. There are about 20 mammalian chemokine receptors, which are 7 transmembrane G-protein coupled receptors (except for so-called atypical receptors) that tend to bind chemokines from one subfamily. There is a great deal of redundancy in the system because many chemokines can bind to multiple receptors, and many receptors can have multiple chemokines as ligands. While this redundancy makes the system more resilient since a mutation in the gene for one receptor may not lead to a diminished immune response, it also means that medically targeting the chemokine system to reduce inflammation is a complex endeavor that may encompass the need to modulate multiple chemokines, multiple receptors and/or multiple cell types [2].

Chemokine binding to cognate receptors has been the subject of much inquiry and occurs with two sites on the chemokine interacting with two sites on the cognate receptor, leading to receptor activation. The CC chemokine N-loop (from about residues 12–20) and basic residues in the 40s loop bind to the N-terminus of the cognate receptor; subsequently the chemokine N-terminal tail contacts the receptor transmembrane region [1] [Fig. 1A]. Mutation studies on chemokines have found that deletion of the N-terminal tail still allows the chemokine to bind, but not activate, the receptor [3, 4], while mutations to the N-loop and basic 40s loop residues reduce binding affinity [3–6]. Upon receptor activation, the receptor-bearing cells proceed to move up the chemokine concentration gradient, toward the site of injury or infection. While chemokines tend to form oligomeric structures in solution and when bound to GAGs [7–10], most (in particular CC chemokines) bind and activate the receptor in their monomeric form [3, 4, 11].

Before turning to the topic of the modulation of chemokine signaling by pathogens and parasites, we should also note that dysregulation of this pathway can yield an inappropriate or an overly aggressive immune response which can cause or exacerbate a variety of ailments including arthritis, atherosclerosis, and traumatic brain injury [12–14]. Hence, an increased understanding of this complex chemokine communication system may offer strategies to therapeutically dampen the immune response in some situations.

Given the importance of the chemokine signaling system in maintaining surveillance, inflammation, and protection from various types of invasion, other organisms and especially viruses have evolved numerous ways to subvert the chemokine system. For example, some viruses express chemokine analogs that bind chemokine receptors, often (but not always) to antagonize the receptors and stop the response. An example of such a protein is vMIP-II, a viral protein of 72 amino acids that is produced by herpesvirus HHV-8 with a structure very similar to CC chemokines [15]. This protein binds to several chemokine receptors, being an antagonist for CCR1, CCR5, and CXCR4, among others, while apparently agonizing CCR3 and CCR8 [16, 17]. These chemokine analogs have been reviewed by Alcami and Lira [18]. Another strategy used by viruses is to produce chemokine receptor analogs, which are transmembrane proteins that can bind chemokines and sometimes share the ability to signal. Examples of these include ORF74, produced by Kaposi's sarcoma herpesvirus, and US28, encoded by human cytomegalovirus [18].

Another strategy used by pathogens to control the chemokine response is to secrete soluble chemokine binding proteins (CBP), most acting to bind chemokines before they reach their receptors. The use of CBP allows the pathogen to target specific pathways to subvert the host immune response

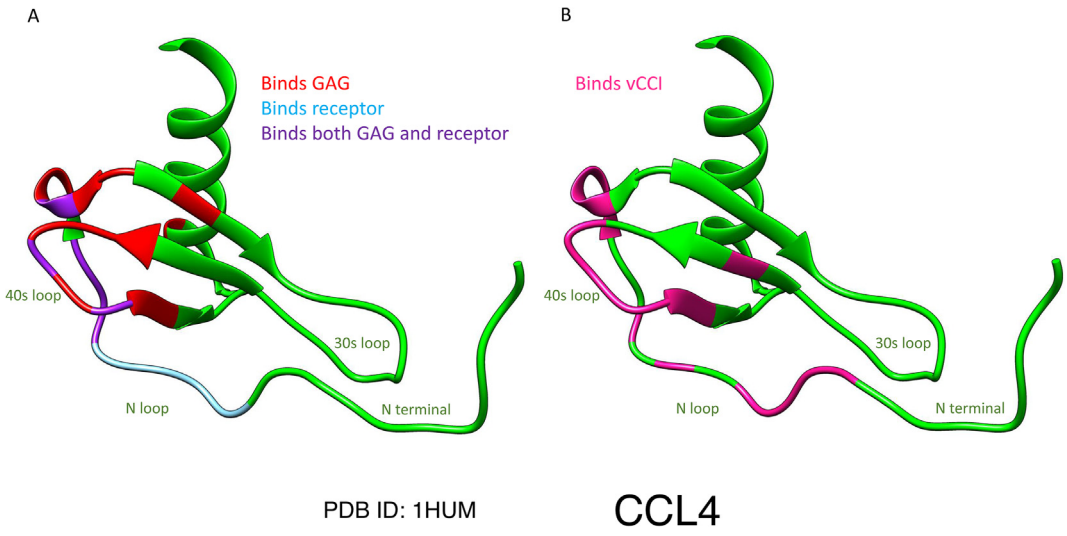

Fig. 1 vCCI binding to CC chemokines shows significant overlap with the chemokine's natural binding contacts. A. Binding contacts made by CC chemokines with the chemokine receptor and with glycosaminoglycans (GAGs). The CC chemokine CCL4 (PDB ID: 1HUM) [87] is used as a typical example. The chemokine is shown in green, with receptor binding contacts shown in light blue. GAG contacts are shown in red. Amino acids that are used both to bind receptors and to bind GAGs are shown in purple [5, 6, 10, 88]. With regard to receptor binding, note that after the initial binding event (using light blue and purple residues), the N-terminus of the chemokine is used to contact the transmembrane regions of the receptor [11]. The chemokine is shown as a monomer although CCL4 forms a dimer under many conditions. B. Binding contacts made by CC chemokines with vCCI. The structure of CCL4 (PDB ID: 1HUM) [87] is shown in green, with residues buried by contact with vCCI shown in deep pink. Contacts were determined from analysis of molecular dynamics simulation of the structure of vCCI in complex with CCL4 (adapted from the structure PDB ID: 2FFK [31]). (Nguyen et al. [69], and subsequent analysis of their data).

[2, 18–21]. Such CBP are expressed by a wide range of poxviruses and herpesviruses [20, 22], and include proteins such as vCCI and M3, respectively. More recently, it has also been discovered that a class of CBP (termed evasins) are used by arthropods such as ticks, that as a group may produce as many as 257 CBP to modulate their host's immune response [23], but note that the arthropod CBP differ in both their structure and mode of function from the viral proteins.

CBP have differing levels of specificity, with some broadly binding multiple sub-families of chemokines, while others bind just one subfamily, or bind only a few chemokines. CBP bind to a variety of different sites on their targets' chemokines. Some CBP bind the GAG-binding region of the chemokine and others bind and block the chemokine's receptor-binding residues or appear to inhibit both functions. Fig. 1B shows the chemokine CCL4 colored to show the binding interaction sites with the CBP vCCI, in comparison to Fig. 1A which shows typical residues used by the chemokine to bind GAGs and its cognate receptor. As described below, a common binding feature of these CBP are loops with up to 50 % acidic residues that bind basic residues that occur in clusters on the chemokine surface. Other areas of electrostatic complementarity further stabilize the CBP-chemokine complex.

Survey of chemokine binding proteins

In this section, we provide a tabular survey of the range of viral and arthropod CBP, listing their chemokine targets, the structural features of their binding, as well as selected data from mutagenesis and/or functional studies on these proteins. This information is listed in Table 1 and the corresponding structures are shown in Fig. 2. Other reviews, with different emphases and scope, are available in the literature [2, 19, 20, 22, 24].

Despite the differences in the CBP noted in the table, there are important structural similarities between groups of these proteins. Several of the poxvirus immune-evading CBP share a conserved β sandwich fold (shown in yellow in Fig. 2 and referred to by Nelson et al. as a "poxvirus immune evasion", or "PIE" domain [21] that is not seen in prokaryotic or eukaryotic proteins (the arthropod CBP Evasin-3 shown in Fig. 2G does not contain a β sandwich since it has only one β sheet). One face of this β sandwich acts as the binding surface for the chemokines [see Figs. 2 and 3]. Another feature seen in several of these proteins is the "acidic loop" facing the binding site which acts as an "arm" to provide additional binding contacts to the chemokine [see Fig. 3] and ranges in size from 25 residues in rabbitpox vCCI to only 4 residues in M3 [Fig. 2E]. Finally, an interesting structural feature that seems to be induced by chemokine binding to CBP is the β strand that is formed in the chemokine itself from chemokine residues 8–14 and that is observed in experimental structures of CBP-chemokine complexes, but not seen in the unbound proteins (see further discussion in section 4.1 below).

The structural and mutation data shown in this table provide numerous independent clues about the specific residue–residue interactions that mediate chemokine-inhibitor binding. However, this data does not on its own constitute a "deciphering of the language" of inhibitor

Table 1 Selection of CBP from different organisms, listing their chemokine targets, their medical relevance, and summarizing the structure and binding information available in the literature.

Name, Origin, and Chemokine Target	Medical/Biochemical relevance	Structural features and mutation effects Figure location (PDB IDs)
vCCI (aka 35K) Organism: Various poxviruses, including rabbitpox virus, cowpox virus, vaccinia virus, variola virus • CC **vCCI (aka EVM1)** Organism: Ectromelia virus (Mousepox virus) • CC	• Ameliorates numerous inflammatory conditions, including arthritis [25] and atherosclerosis in mice [26–28], and allergic inflammatory reactions in guinea pigs [29]. • Effective when used intranasally to decrease airway inflammation in a murine model of asthma [30].	Fig. 2A (**2FFK** [31], **2GRK** [32], **1CQ3** [33]); **(vCCI-CCL4 PDB ID: 2FFK)** [31] • Composed mostly of a β-sandwich fold and has a flexible, highly acidic loop between β strands 2 and 3; or β strands 2 and 4. Forms a 1:1 complex with chemokines. • Length of the acidic loop varies amongst the poxviruses; vCCI uses this loop to interact with key conserved basic residues in the CC chemokines 20s region and 40s loop. • Vaccinia virus vCCI shows a loss of function for mutations E143K or Y80A, and enhanced activity with the mutation R89A [34]. • Mousepox vCCI loses chemokine affinity with the Y69R and the I173R mutations (equivalent to Y80 and I184, respectively in rabbitpox vCCI) [32].
A41 Organism: Vaccinia virus • CC	• Does not inhibit chemokine-induced leukocyte chemotaxis [35]. • Interferes with GAG binding by chemokines [35].	Fig. 2B (**2VGA**) [35] • Has 19 % sequence identity and similar structure to cowpox vCCI [35] • Uses a negatively charged patch in β sheet II to interact with the chemokine's positively charged loops. • Lacks the acidic loop between the N-terminal β strands, found in vCCI. • Binds chemokines less tightly than the vCCI family.
ORFV CKBP Organism: Parapoxviruses • CC • CXC • C	• BPSV CBP (related to OrfV CKBP) reduces skin inflammation in mice [36] and reduces brain inflammation following a stroke in mice [37].	Fig. 2C (**4P5I**, **4ZK9**, **4ZKB**, **4ZKC**) [38] • Exists as a dimer and forms a 2:2 binding stoichiometry with chemokines, unlike the structurally similar A41 and vCCI. • Has a β-sandwich fold along with a small acidic loop between β strands 2 and 3 [38]. • Binds CC chemokines in a similar manner to that used by vCCI. • Contains key binding residues E58, E62, E67, binding to R18 and R24 (CCL2 numbering) on the chemokine. • Has a hydrophobic region that forms an antiparallel β strand with the chemokine N-loop (residues 10–17, CCL2 numbering), which contains the residues F13/Y13 used by the chemokine for receptor engagement [38].
SECRET Domain Organism: CrmB (variola virus) and CrmD (ectromelia virus). • CC • CXC • C • CX3C	• Inhibits arthritis when combined with a TNF binding protein [39]. • Transgenic expression CrmD attenuates gut inflammation in a mouse model of Crohn's disease, likely due both to the TNF-binding ability and the chemokine binding ability of CrmD [40].	Fig. 2D **(CrmD SECRET domain from Ectromelia virus, PDB ID: 3ON9)** [41]**; (CrmD SECRET domain-CX3CL1 PDB ID: 3ONA)** [41] • SECRET domain of CrmD adopts a β sandwich and uses β-sheet I in its interaction with the chemokine, unlike vCCI which uses β-sheet II. • Structure of SECRET domain of CrmD in complex with CX3CL1 shows a relatively small surface area of interaction, with heavy reliance on the basic 40s loop of the chemokine in the binding interaction [41]. • Mutation of the positively charged basic residues in the chemokine (K18 and basic residues in the 40s loop, CX3CL1 numbering) confirms their importance in binding the SECRET domain of CrmD. Corresponding mutations in the SECRET domain (D167A/E169A/D316A) abrogate chemokine binding [41]. • VaV CrmB and EV CrmD found to bind CCL28, CCL25, CXCL12β, CXCL13, and CXCL14 with high affinities, in a study of 43 human chemokines using SPR [42].

Table 1 – (*continued*)

Name, Origin, and Chemokine Target	Medical/Biochemical relevance	Structural features and mutation effects Figure location (PDB IDs)
M3 Organism: Mouse herpesvirus-68 • CC • CXC • C • CX3C	• In mice inhibits experimental autoimmune encephalitis (EAE), a disease model for multiple sclerosis in humans [43]. • Prevents streptozotocin-induced diabetes in mice [44].	Fig. 2E (**PDB ID: 1MKF**) [45]; (**M3-CCL2 PDB ID: 2NZ1, M3-XCL1 PDB ID: 2NYZ**) [46] • Inhibits both the receptor binding and GAG binding functionality of chemokines. • Exists as a dimer and the core of the N-terminal domain (NTD) possesses similar structure to vCCI, although with low sequence identity [45]. • Binds chemokines with 2:2 stoichiometry. • Makes contact with the N-terminal/N-loop receptor-binding portion of the chemokine, starting at around residue 8 of the chemokine and including the critical receptor binding residue CCL2 Y13 and XCL1 V12 [46]. • Contacts basic regions of the chemokine, including R24 (CCL2 numbering), parts of the 30s loop, and the 40s loop region, the same regions used by chemokines to bind glycosaminoglycans [46].
R17 Organism: Rodent herpesvirus Peru (RHVP) • CC • C	No medical application noted in the literature	Fig. 2F(**PDB ID: 4ZKQ**); (**R17-CCL3 PDB ID: 4ZLT**) [47] • Forms a two-domain structure (N-terminal and C-terminal β sandwich domains) connected by a bridging sheet; similar in structure to M3 despite only 8 % sequence identity. • Has 1:1 stoichiometry compared to 2:2 for M3, with different chemokine binding location, despite their structural similarity. • Binds chemokines in a hydrophobic cavity formed by a flexible linker connecting the two domains. • Mutations that remove negatively charged residues from the linker region 266–270 greatly diminish its ability to bind CC chemokines. • Residues of the chemokine involved in binding R17 are very similar to those used to bind vCCI, including F13, S35, and the residues of the chemokine 40s loop such as R45 and N46. • Mutations to the 40s loop of CC chemokines to add positive residues showed increased binding to R17 [47].
Evasin-1,4 **ACA-01** Organism: Arthropod • CC	• Evasins have been shown to reduce inflammation in mouse acute pancreatitis and experimental colitis [48, 49].	Fig. 2G (**Evasin-1 PDB ID: 3FPR**); (**Evasin-1-CCL3 PDB ID: 3FPU**) [50] • Composed of mostly β strands in a "boat" shape. When bound to CCL3, a 1:1 complex is formed. The chemokine sits in the "boat" and contacts both the N- and C-terminal portions of Evasin-1 [50]. • Chemokine contacts include T16, S17, and R18, as well as having a π–π interaction between the F13 of CCL3 (a critical receptor binding residue) and F14 in Evasin-1 [50]. • Evasin-1 uses residues F14 and W89, while Evasin-4, believed to have a similar fold, appears to bind chemokines using different residues, E16 and Y19 [51]. • Evasin ACA-01 has been shown to be sulfated at an N-terminal Tyr, indicating likely sulfation of other evasins [52].
Evasin-3 Organism: Arthropod • CXC	• Inhibits neutrophil chemotaxis [53].	Fig. 2H (**Evasin-3 PDB ID: 6I31**) [54] • 66 amino acid protein, structure determined in the absence of chemokines [53]. • Binds to "ELR" containing CXC chemokines, which are a subset having Glu-Leu-Arg near their N-terminus for receptor engagement. • Glycosylated when produced from mammalian cells; active when produced from *E. coli* without glycosylation.

(*continued on next page*)

Table 1 – (*continued*)

Name, Origin, and Chemokine Target	Medical/Biochemical relevance	Structural features and mutation effects Figure location (PDB IDs)
M-T1, M-T7 Organism: Myxoma virus M-T1: • CC M-T7: • CC • CXC • C	• Both M-T1 and M-T7 have shown some efficacy in pre-clinical trials in suppressing inflammatory responses [55, 56]. • M-T7 has been shown to reduce hyperplasia after vascular injury from angioplasty in both rabbits and rats [56].	**No published structure** • With 40 % amino acid identity with vCCI proteins (the main subject of this review), M-T1 binds CC chemokines at nanomolar levels [57]. • M-T1 can simultaneously bind both glycosaminoglycans and chemokines, potentially allowing localization to sites of inflammation as well as disruption of chemokine function [58]. • M-T7 binds IFN-γ and weakly binds chemokines from three subfamilies [59]. • M-T7 likely binds chemokines via the chemokine GAG binding region, not via their receptor binding region [59], indicating that the action of this binding protein is to disrupt the chemokine gradient rather than to directly disrupt receptor interaction.

recognition of chemokines. One path towards that goal, described in the remainder of this review, is to focus on one class of chemokine inhibitor, assay their binding affinities to a range of chemokines, and then correlate this data with contacts observed in atomistic molecular dynamics simulations of each inhibitor–chemokine pair. The accuracy of the simulations is then validated by experimentally testing proposed mutations predicted in the simulation to increase or decrease binding.

vCCI: a CC chemokine binding protein

In this section we focus on one CBP, vCCI from rabbitpox, to provide a detailed analysis of the structural features of its chemokine binding and to highlight the roles of molecular simulation in elucidating these features. Poxviruses have large genomes and produce a variety of chemokine binding proteins. VCCI, sometimes called p35 or 35K, is a chemokine binding protein made by several poxviruses, including those that infect humans and other mammals. VCCI has been shown to bind dozens of CC chemokines, many with low sequence identity to each other, at nanomolar (or even picomolar) levels [60, 61]. This makes it a particularly intriguing example for the study of protein–protein interactions.

Experimental studies of vCCI-Chemokine binding

Structurally, vCCI resembles several other chemokine binding proteins, being composed of 11 β strands forming a β sandwich configuration [31–33]. Its bound structure reveals that one face of the sandwich contains the binding site, and there is a large, negatively charged loop between β strands 2 and 3 that is used to anchor the CC chemokine in place, as described in more detail in this section below [31, 32]. VCCI is capable of binding more than 80 different CC chemokines across multiple species; however, Burns et al. found no significant binding of vCCI to chemokines from the other three subfamilies [60]. All CC chemokines share a similar tertiary structure composed of three antiparallel β sheets in a Greek key conformation, ending with a C-terminal α helix, but differ greatly in their amino acid sequence and also differ in their cognate receptors. To maintain the specificity for CC chemokines along with the ability to bind such a variable group of proteins, vCCI utilizes both specific amino acids on its binding face, and its highly acidic loop to complement the positively charged residues conserved on chemokines.

VCCI binds CC chemokines in a 1:1 ratio, as shown in Fig. 2A where the structure of vCCI in complex with CCL4 is shown [31]. Key contacts between vCCI and CC chemokines are mediated by negatively charged residues on vCCI, including a long loop composed largely of acidic amino acids. This loop can vary in length, with the rabbitpox vCCI loop being 25 amino acids, while the mousepox (ectromelia) EVM1 loop is only 15 amino acids. These residues and others, including E143 and D141 bind to basic residues on the chemokine. VCCI also forms a hydrophobic interaction with F13 on the chemokine, a position typically containing a large hydrophobic residue in most CC chemokines, that is critical for binding its cognate receptor. Residues 8–14 of the CC chemokine interact with residues 180–186 of vCCI, forming an additional antiparallel β strand upon binding. Interestingly, this formation of a new β strand in the "N-loop" of the chemokine upon complex formation has also been observed in several other chemokine binding proteins, including in M3 binding to CCL2 [45], Evasin-1 binding to CCL3 [50], and ORFV CKBP binding to CCL2 [38]. While not labeled as a β strand in the structure for vCCI with CCL4 in Fig. 2A, the additional β strand has been observed in MD simulations with vCCI bound to several chemokines [62].

Early studies of vCCI-chemokine interactions involved mutating residues on the chemokine and testing these for changes in binding affinity to determine the involvement of the residue in the interaction. Two such studies tested mutations on CCL2 by surface plasmon resonance and ELISA assays, and both found that Y13A, R18A, and R24A (as well as R24E) significantly reduced affinity to vCCI [63, 64]. These residues have been previously shown to also be utilized for chemokine receptor binding [6], indicating that vCCI blocks chemokine signaling by obscuring residues involved in receptor binding.

Our group found similar interactions in these conserved residues in a variant of CCL4. This work determined the structure of vCCI bound to CCL4 using NMR [31] and indicated that R18 interacts with D141 and E143 of vCCI, both found on the binding face of the β sandwich (Supplementary Fig. 1C). In the vCCI:CCL4 structure, the residue F24 (analogous to R24 in CCL2), along with K45 and R46 (both mutated to alanine in the structural study to reduce aggregation) were found near the acidic loop of vCCI (Supplementary Fig. 1B shows the simulated structure of wild type CCL4 bound to vCCI including its interactions with the acidic loop, with residues 24, 45, and 46 highlighted.). In aligned sequences for multiple CC chemokines, at least one positive charge is found in the corresponding 24/45/46 residues. The distribution of acidic residues in the vCCI loop allows it to find complementary charges on the 20s and 40s loop of chemokines. In later work, we confirmed the importance of charged basic residues on the chemokine by mutating these residues in CCL11 (R22A and K44A). Mutating only one of these residues results in a 1.5- to 2-fold decrease in affinity as measured by fluorescence, mutating both results in a 4.8-fold decrease, and mutating both along with R16A (equivalent to R18 in CCL4) leads to a 134-fold decrease [61].

Structural studies also showed that F13 of CCL4 (Y13 in CCL2) fits in a hydrophobic pocket between β sheets I and II of vCCI. As noted in a sequence analysis by Ziarek et al. of 24 human CC chemokines, 9 had a Phe in this position, with other residues generally being large hydrophobics like Leu and Tyr [65]; this residue generally has a role in both in receptor binding and in mediating chemokine dimerization [4, 5]. Mutation to alanine in this position results in an approximately 10-fold decrease in affinity for vCCI [63, 64], likely due to reduced interactions with the hydrophobic pocket of vCCI, formed by conserved residues V185 and Y217 (Supplementary Fig. 1D).

Work on CCL2 also found that K49, when mutated to alanine, showed an increase in binding affinity to vCCI [63, 64]. This is often a conserved basic residue in CC chemokines (K48 in CCL4, K47 in CCL11). When bound to vCCI, this residue packs closely with Y80 and R89, likely causing steric crowding and/or poor electrostatic interactions due to the positive charges of the two basic residues (see Supplementary Fig. 2). Fremont et al. replaced Y69 of EVM1 (Y80 in vCCI) with a large, positive residue, correctly hypothesizing that it would drastically reduce chemokine binding [32]. Correspondingly, it was proposed that mutation of either Y80 or R89 to the small amino acid alanine in vCCI would likely reduce this clash and improve overall binding. White et al. [34] tested this hypothesis by separately mutating Y80 and R89 in vCCI to see if replacing these residues with alanine would result in better chemokine binding by vCCI and therefore lower chemokine function. Per their expectations, R89A was found to increase chemokine binding (and thereby block the activity of CCL5, which was the chemokine used in their functional assays). However, rather than enhancing chemokine binding, the Y80A mutation paradoxically resulted in loss of the ability of vCCI to inhibit CCL5 activity, presumably because the Y80A vCCI variant was no longer able to bind the chemokine [34]. The question of why the Y80A vCCI variant unexpectedly has weaker chemokine binding is currently being addressed computationally and in ongoing experiments [66–68].

Computational simulations of vCCI-Chemokine binding

The experimental data described in the previous section provided myriad separate clues about the roles of individual residues involved in vCCI-chemokine binding. Computational molecular modeling can provide a framework to holistically evaluate the contributions of each residue to this binding interaction. Recently we published a combined experimental and computational study of the binding of vCCI to the chemokine CCL4 and the virally produced chemokine analog vMIP-II [69]. NMR analysis showed an overall similar binding by vCCI to the two proteins, and fluorescence studies found that vCCI:vMIP-II had a higher binding affinity than vCCI binding to an actual mammalian chemokine, CCL4. Molecular dynamics simulations (see Appendix for a brief overview of relevant molecular simulation techniques) were performed on these complexes, as well as on a complex with the CCL4 mutant that was used to solve the original structure of the vCCI:CCL4 complex (K45A/R46A/K48A). An analysis was performed of the type and duration of the vCCI-chemokine interactions. These simulations showed that the vCCI:vMIP-II structure had more interprotein hydrogen bonds and interface surface area than vCCI:CCL4, which in turn had more extensive contacts than the vCCI:CCL4 mutant. These results qualitatively corroborated the measured binding affinities, but importantly also produced residue-level "maps" of the interprotein interactions which mediate the binding. To give some examples of structural results noted in this study: the chemokine residue R18 is shown to be important in the binding of both vMIP-II and CCL4; vCCI S182 was seen to have a persistent hydrogen bond to C51; and the vCCI I184 (rabbitpox numbering) which earlier studies in mousepox [32] had suggested caused unfavorable interactions, was instead seen in the MD simulations to interact with I41 and C51 in vMIP-II [69].

In addition to providing atomic-level details of the binding in experimentally realized complexes, simulations can also be applied to "hypothetical" complexes, to predict the structure and qualitatively estimate the binding strength. For example, the chemokine CCL17 is one of the few CC chemokines that does not bind well to vCCI [60], likely because CCL17 lacks several of the positively charged residues that have been shown to be important in a vCCI:chemokine complex, including lacking basic residues at positions 18, 45, and 46 (CCL4 numbering). Molecular dynamics simulations of the vCCI:CCL17 complex yield results that can be compared to simulations of vCCI bound to CCL4 and vMIP-II [62]. Fig. 3 shows the contacts and final bound structures from molecular dynamics simulations of vCCI bound to CCL4 and CCL17. The images show the solvent-accessible surface of each protein superimposed on its secondary structure given in the usual "cartoon" format. The contact regions for both proteins are shaded in purple. This illustrates the similarities and differences in the binding of these two chemokines. Both chemokines have multiple contacts to the face of β sheet II of vCCI and all along the acidic loop which wraps over both chemokines. Comparing the two simulated structures, both chemokines obscure nearly the same residues of the vCCI β sheet II

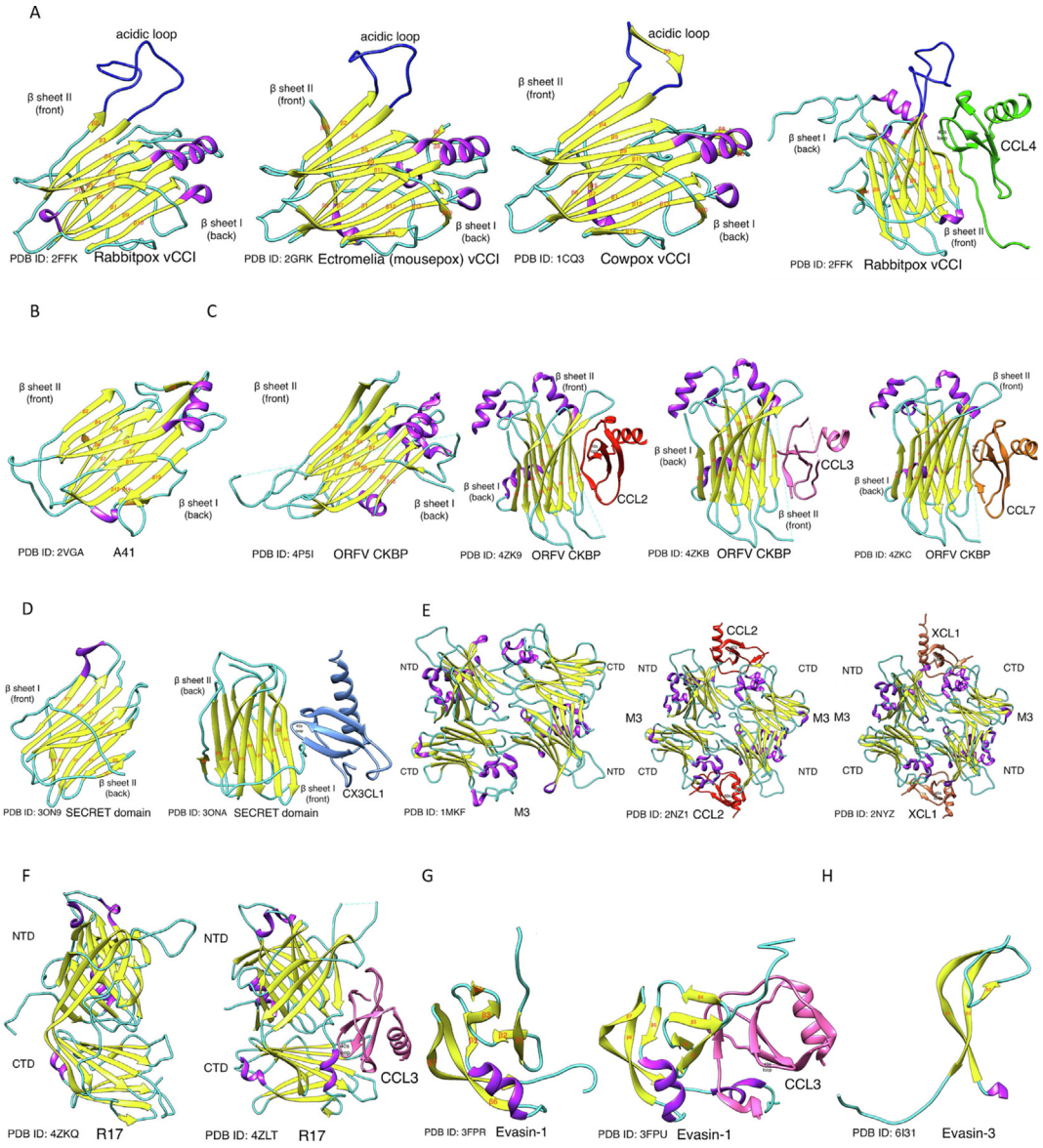

Fig. 2 The structures of vCCI and other chemokine binding proteins, and their complex with chemokines. Chemokine binding proteins are shown in yellow ribbons with purple helices and blue loops. A: Poxvirus CC chemokine inhibitors. (Left) Three unliganded vCCI: rabbitpox vCCI (PDB ID: 2FFK [31], ectromelia (mousepox) vCCI (PDB ID: 2GRK) [32], cowpox vCCI (PDB ID: 1CQ3) [33], all shown in the same orientation with acidic loop on the top and β sheet II binding site in the front. Because no unliganded structure of rabbitpox vCCI is available, the "unliganded" rabbitpox vCCI shown here is derived from the vCCI:CCL4 complex and is shown without its ligand for comparison. (Right) rabbitpox vCCI in complex with a CCL4 variant (PDB ID: 2FFK), showing how the rabbitpox vCCI acidic loop and its β sheet II interact with CCL4. B: The structure of vaccinia A41(PDB ID: 2VGA) [35], which is very similar to the structure of vCCI, but does not bind chemokines as tightly as the vCCI family [35]. C: Orf virus ORFV CKBP has a similar β sandwich structure and acidic loop as vCCI, and binds CC chemokines in a similar manner as vCCI [38]. ORFV CKBP has been found to be a dimer and forms a 2:2 binding stoichiometry with chemokines, but we show the monomer to illustrate the similarity to vCCI. From left to right is shown unliganded ORFV CKBP (PDB ID: 4P5I) [38]; ORFV CKBP bound to CCL2 (PDB ID: 4ZK9) [38]; ORFV CKBP bound to CCL3(PDB ID: 4ZKB) [38]; ORFV CKBP bound to CCL7(PDB ID: 4ZKC) [38]. D: The ectromelia virus-encoded SECRET domain of CrmD (Left) (PDB ID: 3ON9) [41] and its complex with chemokine CX3CL1 (Right, blue) (PDB ID: 3ONA) [41]. While the SECRET domain has a similar β sandwich structure as vCCI, it uses β sheet I rather than β sheet II to interact with the chemokine [41]. E: (Left) Murine gammaherpesvirus68-encoded M3 forms a two-domain β sandwich (PDB ID: 1MKF) [45]. (Right) the complex of M3 with CCL2 (red) (PDB ID: 2NZ1) [46] and XCL1 (salmon color, PDB ID: 2NYZ [46]. The stoichiometry of both of these complexes are 2:2. F: (Left) The structure of R17 (PDB ID: 4ZKQ) [47], encoded by rodent herpesvirus Peru (RHVP), has a similar 2-domain β sandwich structure as M3, but (Right) the binding location of the chemokine CCL3 (pink) is different (PDB ID: 4ZLT) [47]. G: Evasin-1, a chemokine binding protein from tick salivary gland. (Left) unbound (PDB ID: 3FPR) [50]. (Right) Evasin-1 in complex with CCL3 (pink, PDB ID: 3FPU) [50]. H: Evasin-3 (PDB ID: 6I31) [54], a chemokine binding protein from tick salivary glands. This protein has a knottin scaffold structure which is necessary for different CXC-chemokine-binding activities [54].

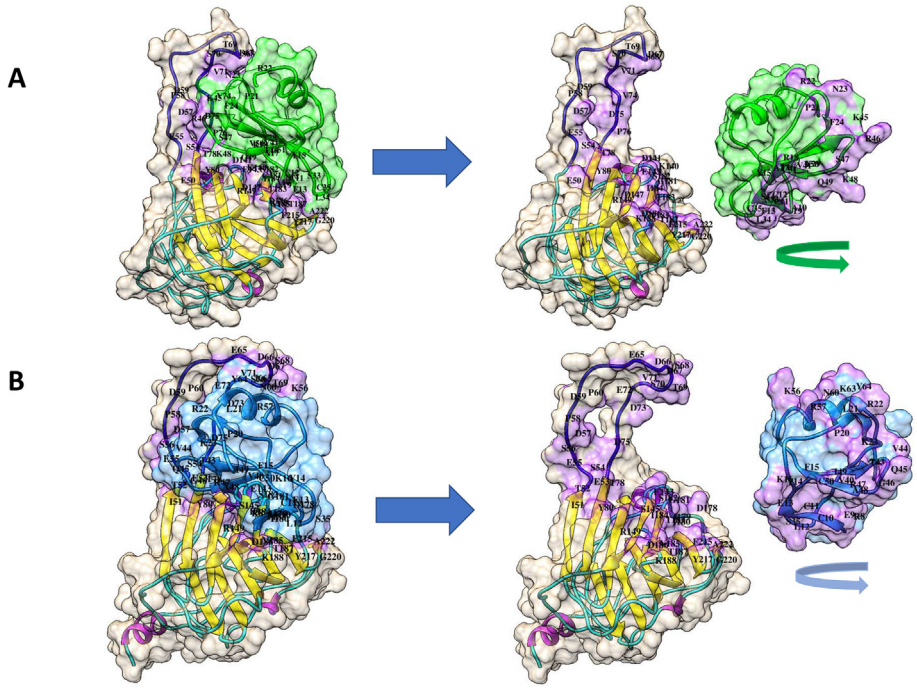

Fig. 3 Interface of vCCI and its chemokine ligands as predicted by molecular dynamics simulations. The surface area is shown for (A) vCCI when bound to CCL4 and (B) vCCI when bound to CCL17. The structure used in A comes from the PDB ID 2FFK [31], in which the CCL4 ligand was mutated back to wildtype and molecular dynamics was run for 1μs. In B, the vCCI:CCL17 structure was built by modeling the complex, starting with 2FFK and replacing the chemokine by aligning the Cα backbone. To visualize the intermolecular interactions, each component has been moved apart and rotated to reveal the binding face. vCCI (beige) is on the left, the chemokine ligand is on the right (green for the CCL4, blue for CCL17). The contact surface area between vCCI and each chemokine is colored in purple. The residues involved in the interface on both vCCI and the chemokine are labeled. Contact surface area identified on the CCL17 α helix suggests non-canonical binding with the vCCI acidic loop compared to other chemokines.

face. The differences appear in how the acidic loop of vCCI binds the chemokine. In complex with CCL4, the lower region of the vCCI acidic loop (residues 54–59) contacts the 40s loop of the chemokine, while the middle residues of the vCCI loop (residues 67–71) interact with the chemokine's 20s region. In the simulation with CCL17, the lower region of the vCCI loop (residues 55–60) contacts the 20s region and the 40s loop of CCL17, while the middle residues of the vCCI loop interact with the α helix of the chemokine instead.

The persistent vCCI-chemokine contacts for vCCI bound to CCL17, as well as for vCCI bound to CCL4, mutant CCL4, and vMIP-II [69] are shown in Fig. 4. In each diagram, the line at the top represents the sequence of residues in vCCI and the line at the bottom represents the residues in the chemokine. The colored lines between the vCCI and the chemokines show persistent contacts during the molecular dynamics simulation, and these are color-coded by the fraction of the simulation time they are present, with the green line indicating the most persistent contacts. All four chemokines show extensive, persistent contacts between the N-terminal region of the chemokine (residues 8–14) and β strand 8 on vCCI (residues 180–187). But clear differences arise in the number and persistence of contacts from CCL17 to the vCCI acidic loop (residues 57–75) and other residues on β strand 7 (residues 143–149), compared to the other three chemokines. The fewer, but more persistent, contacts of the vCCI loop to CCL17 suggest the loop becomes locked in a particular conformation with the α helix due to the limited number of charged residues available for it to bind. In contrast, the acidic loop can move between the key charged residues along the 20s region and the 40s loop in other chemokines, resulting in more interactions [62].

Fig. 5 shows the buried surface area for vCCI and several chemokines as determined by MD simulations. This type of representation illustrates the shared binding face on vCCI. One region of note, residues 180–186 of vCCI, shows identical occlusion (calculated based on the accessibility of the residues to a water-sized molecular probe) from each chemokine. Computer visualizations and secondary structure analysis of MD simulations of this region show each of the chemokines forming an additional β strand aligned with chemokine residues 8–14 [see Fig. 3 and Supplementary Fig. 4]. As noted previously in sections 3 and 4.1, this feature, observed in simulation, appears to be common in the experimentally determined structures of binding of chemokines by several CBP, including M3, Evasin-1, and ORFV [38, 45, 50]. As in the results given in Figs. 3–5, this shows that CCL17 has distinct differences in its binding structure compared to the other chemokines simulated. This chemokine causes a similar pattern of buried surface area on the residues of vCCI as do the other chemokines. However, the buried surface area on the CCL17 itself is notably different from that on other

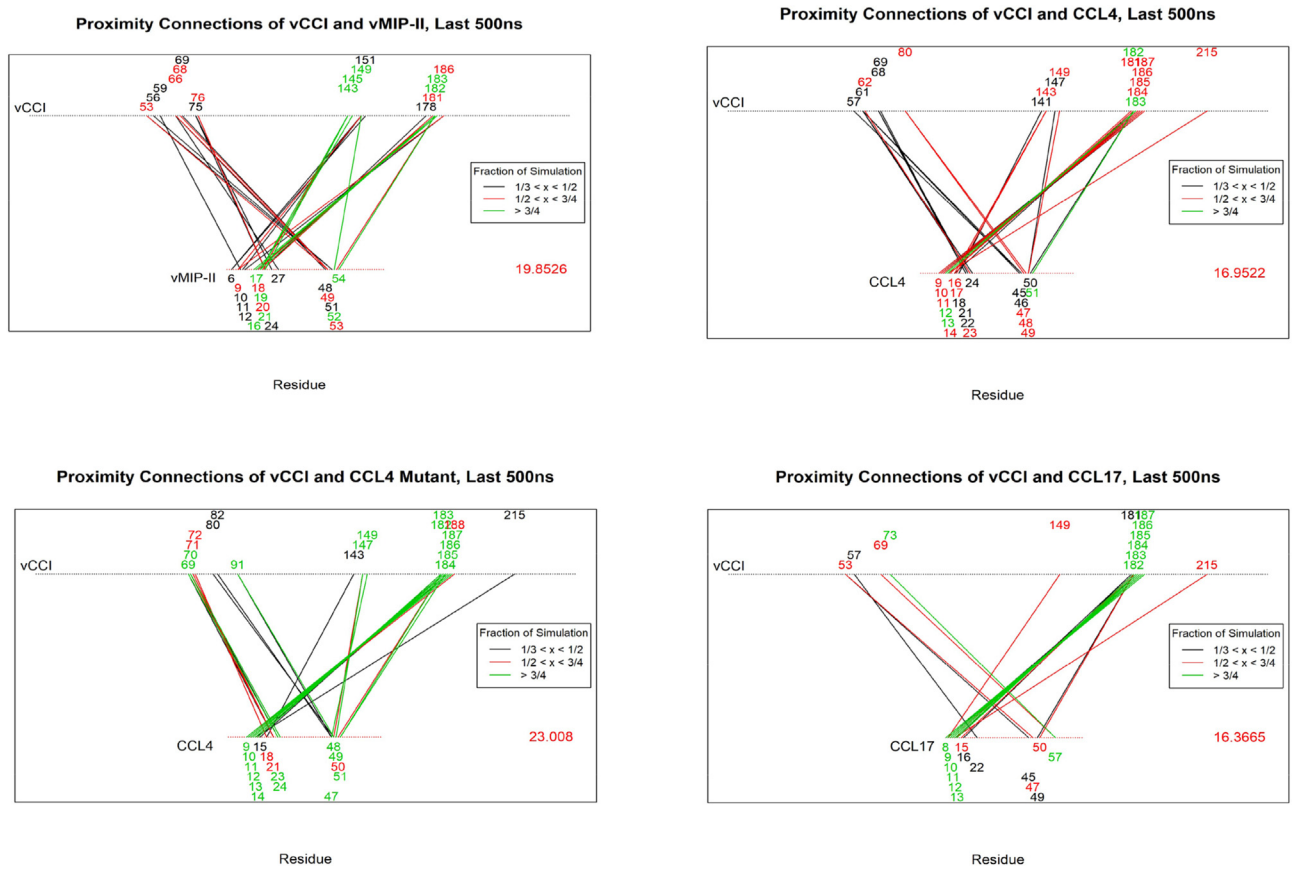

Fig. 4 Contact maps for vCCI:chemokine interactions. Contact maps show the residues in close proximity between vCCI and the designated chemokine. Analysis was performed on the last 500ns of the 1μs simulations to allow the system to equilibrate. The top horizontal line in each figure represents the sequence of vCCI, from amino acids 1–242. The bottom horizontal line represents the amino acid sequence of each chemokine, ranging from residue 1 to about 70, depending on the chemokine. Each transecting line indicates a contact between vCCI and the chemokine during the last 500 ns of the simulation. The color of the line indicates the fraction of the simulation time the two residues are within 2.8 Å of each other, ranging from black (in contact for a third to a half of the simulation; 167–250ns); red (in contact for a half to three-fourths of the simulation; 250–375ns); and green (in contact for more than three-fourths of the simulation; more than 375ns). The numbers above and below the horizontal lines list the residue numbers of vCCI and the chemokine, respectively, that are involved in an interaction. The color of the number is representative of the most persistent interaction it is a part of, matching the coloring used for the transecting lines. The number in the lower right of each graph is the sum of the fraction of time during the simulation that the indicated interactions are observed, where a higher number indicates more persistent and/or a larger total number of interactions throughout the simulation [62].

chemokines when bound to vCCI. Unlike the other three chemokines shown, CCL17 has several residues in the C-terminal α-helix in contact with vCCI. This distinctive binding pattern has not yet been experimentally verified, but it is reasonable to infer that the need for the vCCI acidic loop to be highly extended to bind to the CCL17 helix may lead to reduced binding for CCL17 compared to other CC chemokines.

Prospects for engineering CBP specificity and affinity

As described in section 4, many studies have investigated amino acids on the chemokine that affect its binding to a CBP, particularly with vCCI [61, 63, 64]. Perhaps more relevant for the practical use of CBP in medical applications are investigations to add chemokine binding functionality to this medically relevant protein itself [39] or to study changes in CBP that affect their ability to bind particular chemokines. Structural studies have guided mutations in vCCI-like proteins to determine important features for chemokine binding [32] as well as to allow the successful construction of a variant (R89A) that increases the potency of vCCI [34]. Another study used computer modeling to obtain a structural model of Evasin-4 in complex with a chemokine, followed by phage display to confirm binding determinants suggested by the model [51]. This was a successful marriage of computation and experiment, although the authors expressed disappointment that

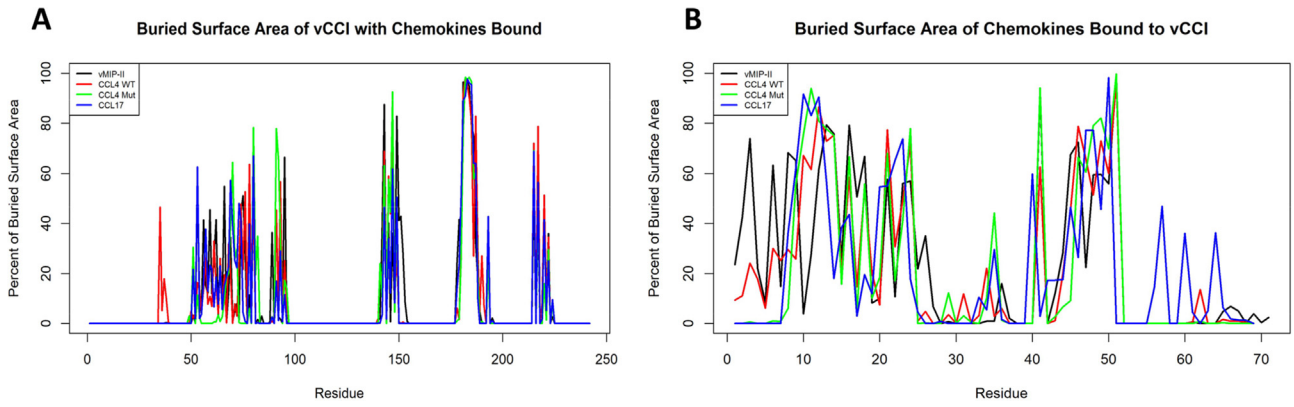

Fig. 5 Buried surface area of vCCI and chemokines when forming a vCCI:chemokine complex. The percent of buried surface area of each residue is shown for (A) vCCI and (B) selected CC chemokines. The x-axis represents the amino acid sequence of each protein; the y axis represents the percent of that amino acid that is buried during the last 500ns of the 1μs simulation of the complex. The percent of buried surface area is based on the ratio between the buried surface area (when bound) and the accessible surface area (when in solution). Each colored line represents a complex between vCCI and a separate chemokine, with vMIP-II, CCL4 WT, CCL4 Mut, and CCL17 shown in black, red, green, and blue respectively. (A) shows that buried surface area for vCCI is largely the same regardless of the chemokine bound, while (B) shows greater variability in amino acids making contact with vCCI, depending on the chemokine. "CCL4 Mut" is the K45A/R46A/K48A variant of CCL4. Similarities across complexes, such as the 180–186 peak in (A), indicate conserved regions involved in chemokine binding. Alternatively, differences in buried surface area, such as the peaks from 55 to 65 for CCL17 in (B), can reveal unique binding patterns not utilized by the other complexes [62].

this work did not lead to the successful design of a potent chemokine inhibitor [19].

We contend that the synergy of structural biology, biochemical experiments, and computer modeling will lead to a more nuanced understanding of CBP-chemokine interactions, which can, in turn, allow molecular engineering of CBP and chemokines with novel binding strength and specificity. These can be tested experimentally, and iteratively optimized until a particular goal is achieved. In ongoing work, we are investigating the complex between vCCI and CCL17. As noted in the previous section, vCCI does not bind CCL17 well [60], likely because CCL17 lacks several of the important basic residues that have been shown to confer affinity to vCCI. A highly specific CCL17-binding protein would be valuable in the study of certain diseases because this chemokine recruits Th2 cells during the inflammatory response in several medical conditions, including allergic asthma [70, 71]. Therefore, we plan to use a combination of simulation and experimental work to make a variant vCCI that has high affinity to CCL17. The goal is to modify only vCCI, not CCL17, so that the modified CBP can bind wild type CCL17 as proof of concept that this design technique could be used in a real-world application.

Overall, the long co-evolution of viruses and parasites with their hosts has led to a unique family of proteins, CBP, that subvert the mammalian immune system by binding to chemokines, thereby impeding the function of some host immune cells. Due to this binding ability, CBP have been shown to have remarkable anti-inflammatory properties *in vitro* and *in vivo*, with work ongoing in several labs to translate their function into useful therapeutics [19, 24, 39]. These CBP often share structural features and bind conserved regions of the chemokines, particularly basic residues and those residues involved in receptor binding and GAG binding. A greater understanding of how CBP bind their chemokine ligands can be pursued by a combination of computational and experimental work, with outcomes that may include altered or tailored specificity in chemokine binding.

Appendix: computer simulations of protein–protein binding

As has been described here, viruses and other parasites make a variety of chemokine binding proteins that can be studied to provide a wealth of knowledge about the details of protein–protein interactions. These interactions can inform future studies of other proteins and can be used to make mutations to fine-tune the activity of a particular chemokine binding protein. Given the wealth of structural and biochemical data now available for several of these proteins, computational analysis can be a major tool in their study, leading to testable hypotheses about modes of interactions carried out by CBP and even proposing new mutations to tune binding specificity.

Computer analyses play myriad roles in structural biology and biochemistry, from bioprospecting sequence data for novel genes [72] (including a study to identify evasin-like proteins in tick genomes [23]) to identifying protein–protein binding inhibitors [73]. A potentially profound role for computers is the atomic-scale simulation of biomolecular structure and function, which in principle could elucidate the biochemical mechanisms at exquisite spatial and temporal scales [74]. The most accurate molecular simulations solve the equations of quantum mechanics to predict molecular structures, interaction energies, and even reaction rates, but such

methods are presently too computationally costly to be routinely applied to biochemical questions. Instead, so-called classical molecular dynamics (MD) methods are typically used, where each atom is treated as a classical particle typically carrying a partial charge and bound to other atoms by springs (a detailed introduction to MD algorithms has been published by Frenkel and Smit [75]). The so-called "force fields" used in MD simulations include electrostatic and van der Waals interactions that represent the whole range of molecular interactions, including hydrogen bonds, salt bridges, and hydrophobic contacts. These simulations produce "trajectories" in the form of 3D movies of the motions of every atom in the system during the simulation time. There are inherent limitations to classical MD, especially its inability to directly model chemical reactions, including acid-base chemistry, but despite these limitations, classical MD is emerging as a key tool for studying biochemical processes including protein folding and protein-ligand binding [76, 77]. Improvements in computer speeds and MD algorithms have increased the size and timescale of feasible calculations to the point where multi-microsecond simulations of complete proteins and their immediate surroundings are routine and the longest protein MD simulations run into the millisecond domain [78].

For the specific question of studying and engineering protein–protein interactions, MD has two primary uses. First, MD simulations can generate trajectories containing realistic conformations of the molecular system that can be analyzed to show the location and persistence of electrostatic, hydrophobic, and hydrogen bond interactions between the two proteins, as well as changes in the secondary and tertiary structure of the proteins, as was described in section 4.2 above. For most protein systems, such simulations are sufficiently easy to set up and are fast enough on inexpensive workstations that it is possible to routinely run many simulations of different protein–protein binding pairs. This allows the computational "mapping" of differences in the interactions between different binding partners and different protein isoforms. A recent review article describes many examples of the complementarity of molecular modeling and experimental structural biology for the binding of chemokines to their natural targets as well as to small-molecule inhibitors [79].

Another at least potential use of simulation is for the prediction of absolute and/or relative binding free energies between proteins [80]. These simulations can in principle yield binding free energies accurate to a few kcal/mole, but there are still many challenges to routine free energy binding calculations [81]. Nevertheless, improvements in computer speeds, simulation algorithms, and force fields, are making calculations of relative ligand-protein binding free energies increasingly accurate and feasible, especially for relatively small, "drug size" ligands [82]. The most established method for calculating binding free energies is "free energy perturbation" (FEP) also known as "alchemical perturbation" which involves the computational transformation of a molecule or molecular fragment into another molecule [83]. Although the FEP process is not possible in the physical world, this transformation has the same free energy change as a thermodynamic cycle that first unbinds the first ligand and then binds the second. The routine calculation of accurate protein–protein binding free energies by FEP is hampered by the size and flexibility of protein ligands, but recent, carefully validated studies demonstrate that accurate results are achievable [84]. In addition to free energy perturbation methods, several promising new techniques for calculating the binding free energies are being developed, including fragment-based methods [85] and machine learning methods [86] that offer the promise that protein–protein binding energy calculations will become routine and accurate.

Conflicts of interest

The authors declare that they have no competing interests.

Acknowledgments

Funding was provided by the Army Research Office (W911NF2010268). This work was partially supported by the National Science Foundation through the NSF-CREST: Center for Cellular and Bio-molecular Machines at the University of California, Merced (NSF-HRD-1547848). This work used the Extreme Science and Engineering Discovery Environment (XSEDE), which is supported by National Science Foundation grant number ACI-1548562. Logistical support for this project was provided by the UC Merced Health Science Research Institute. Protein figures were made with Chimera package version 1.13.1 from the Resource for Biocomputing, Visualization, and Informatics at the University of California, San Francisco [89] (supported by NIH P41 RR001081).

Appendix A. Supplementary data

Supplementary data to this article can be found online at https://doi.org/10.1016/j.bj.2021.07.004.

REFERENCES

[1] Bhusal RP, Foster SR, Stone MJ. Structural basis of chemokine and receptor interactions: key regulators of leukocyte recruitment in inflammatory responses. Protein Sci 2020;29:420–32.
[2] Stone MJ, Hayward JA, Huang C, Huma ZE, Sanchez J. Mechanisms of regulation of the chemokine-receptor network. Int J Mol Sci 2017;18:342.
[3] Laurence JS, Blanpain C, De Leener A, Parmentier M, LiWang PJ. Importance of basic residues and quaternary structure in the function of MIP-1β: CCR5 binding and cell surface sugar interactions. Biochemistry 2001;40:4990–9.
[4] Paavola CD, Hemmerich S, Grunberger D, Polsky I, Bloom A, Freedman R, et al. Monomeric monocyte chemoattractant protein-1 (MCP-1) binds and activates the MCP-1 receptor CCR2B. J Biol Chem 1998;273:33157–65.
[5] Laurence JS, Blanpain C, Burgner JW, Parmentier M, LiWang PJ. CC chemokine MIP-1β can function as a monomer and depends on Phe13 for receptor binding. Biochemistry 2000;39:3401–9.
[6] Hemmerich S, Paavola C, Bloom A, Bhakta S, Freedman R, Grunberger D, et al. Identification of residues in the

monocyte chemotactic protein-1 that contact the MCP-1 receptor, CCR2. Biochemistry 1999;38:13013–25.
[7] McCornack MA, Cassidy CK, LiWang PJ. The binding surface and affinity of monomeric and dimeric chemokine macrophage inflammatory protein 1β for various glycosaminoglycan disaccharides. J Biol Chem 2003;278:1946–56.
[8] Deshauer C, Morgan AM, Ryan EO, Handel TM, Prestegard JH, Wang X. Interactions of the chemokine CCL5/RANTES with medium-sized chondroitin sulfate ligands. Structure 2015;23:1066–77.
[9] Wang X, Watson C, Sharp JS, Handel TM, Prestegard JH. Oligomeric structure of the chemokine CCL5/RANTES from NMR, MS, and SAXS data. Structure 2011;19:1138–48.
[10] Lau EK, Paavola CD, Johnson Z, Gaudry JP, Geretti E, Borlat F, et al. Identification of the glycosaminoglycan binding site of the CC chemokine, MCP-1: implications for structure and function in vivo. J Biol Chem 2004;279:22294–305.
[11] Zheng Y, Han GW, Abagyan R, Wu B, Stevens RC, Cherezov V, et al. Structure of CC chemokine receptor 5 with a potent chemokine antagonist reveals mechanisms of chemokine recognition and molecular mimicry by HIV. Immunity 2017;46:1005–17. e5.
[12] White GE, Iqbal AJ, Greaves DR. CC chemokine receptors and chronic inflammation–therapeutic opportunities and pharmacological challenges. Pharmacol Rev 2013;65:47–89.
[13] Wells TNC, Power CA, Shaw JP, Proudfoot AEI. Chemokine blockers - therapeutics in the making? Trends Pharmacol Sci 2006;27:41–7.
[14] Hellewell S, Semple BD, Morganti-Kossmann MC. Therapies negating neuroinflammation after brain trauma. Brain Res 2016;1640:36–56.
[15] LiWang AC, Wang ZX, Sun Y, Peiper SC, LiWang PJ. The solution structure of the anti-HIV chemokine vMIP-II. Protein Sci 1999;8:2270–9.
[16] Kledal TN, Rosenkilde MM, Coulin F, Simmons G, Johnsen AH, Alouani S, et al. A broad-spectrum chemokine antagonist encoded by Kaposi's Sarcoma-associated herpesvirus. Science 1997;277:1656–9.
[17] Szpakowska M, Chevigne A. vCCL2/vMIP-II, the viral master KEYmokine. J Leukoc Biol 2016;99:893–900.
[18] Alcami A, Lira SA. Modulation of chemokine activity by viruses. Curr Opin Immunol 2010;22:482–7.
[19] Proudfoot AEI, Bonvin P, Power CA. Targeting chemokines: pathogens can, why can't we? Cytokine 2015;74:259–67.
[20] Heidarieh H, Hernáez B, Alcamí A. Immune modulation by virus-encoded secreted chemokine binding proteins. Virus Res 2015;209:67–75.
[21] Nelson CA, Epperson ML, Singh S, Elliott JI, Fremont DH. Structural conservation and functional diversity of the poxvirus immune evasion (PIE) domain superfamily. Viruses 2015;7:4878–98.
[22] González-Motos V, Kropp KA, Viejo-Borbolla A. Chemokine binding proteins: an immunomodulatory strategy going viral. Cytokine Growth Factor Rev 2016;30:71–80.
[23] Hayward J, Sanchez J, Perry A, Huang C, Rodriguez Valle M, Canals M, et al. Ticks from diverse genera encode chemokine-inhibitory evasin proteins. J Biol Chem 2017;292:15670–80.
[24] Yaron JR, Zhang L, Guo Q, Burgin M, Schutz LN, Awo E, et al. Deriving immune modulating drugs from viruses—a new class of biologics. J Clin Med 2020;9:972.
[25] Buatois V, Fagète S, Magistrelli G, Chatel L, Fischer N, Kosco-Vilbois MH, et al. Pan-CC chemokine neutralization restricts splenocyte egress and reduces inflammation in a model of arthritis. J Immunol 2010;185:2544–54.
[26] Ali ZA, Bursill CA, Hu Y, Choudhury RP, Xu Q, Greaves DR, et al. Gene transfer of a broad spectrum CC-chemokine inhibitor reduces vein graft atherosclerosis in apolipoprotein E-knockout mice. Circulation 2005;112:235–41.
[27] Bursill CA, McNeill E, Wang L, Hibbitt OC, Wade-Martins R, Paterson DJ, et al. Lentiviral gene transfer to reduce atherosclerosis progression by long-term CC-chemokine inhibition. Gene Ther 2009;16:93–102.
[28] Bursill CA, Choudhury RP, Ali Z, Greaves DR, Channon KM. Broad-spectrum CC-chemokine blockade by gene transfer inhibits macrophage recruitment and atherosclerotic plaque formation in apolipoprotein E-knockout mice. Circulation 2004;110:2460–6.
[29] Alcami A, Symons JA, Collins PD, Williams TJ, Smith GL. Blockade of chemokine activity by a soluble chemokine binding protein from vaccinia virus. J Immunol 1998;160:624–33.
[30] Dabbagh K, Xiao Y, Smith C, Stepick Biek P, Kim SG, Lamm WJ, et al. Local blockade of allergic airway hyperreactivity and inflammation by the poxvirus-derived pan-CC-chemokine inhibitor vCCI. J Immunol 2000;165:3418–22.
[31] Zhang L, Derider M, McCornack M, Jao S-C, Isern N, Ness T, et al. Solution structure of the complex between poxvirus-encoded CC chemokine inhibitor vCCI and human MIP-1beta. Proc Natl Acad Sci U S A 2006;103:13985–90.
[32] Arnold PL, Fremont DH. Structural determinants of chemokine binding by an ectromelia virus-encoded decoy receptor. J Virol 2006;80:7439–49.
[33] Carfi A, Smith CA, Smolak PJ, McGrew J, Wiley DC, Carfí A, et al. Structure of a soluble secreted chemokine inhibitor vCCI (p35) from cowpox virus. Proc Natl Acad Sci USA 1999;96:12379–83.
[34] White GE, Mcneill E, Christou I, Channon KM, Greaves DR. Site-directed mutagenesis of the CC chemokine binding protein 35K-fc reveals residues essential for activity and mutations that increase the potency of CC chemokine blockade. Mol Pharmacol 2011;80:328–36.
[35] Bahar MW, Kenyon JC, Putz MM, Abrescia NGA, Pease JE, Wise EL, et al. Structure and function of A41. a Vaccinia Virus Chemokine Binding Protein 2008;4:e5.
[36] Sharif S, Nakatani Y, Wise L, Corbett M, Real NC, Stuart GS, et al. A broad-spectrum chemokine-binding protein of bovine papular stomatitis virus inhibits neutrophil and monocyte infiltration in inflammatory and wound models of mouse skin. PloS One 2016;11:e0168007.
[37] Lee S, Chu HX, Kim HA, Real NC, Sharif S, Fleming SB, et al. Effect of a broad-specificity chemokine-binding protein on brain leukocyte infiltration and infarct development. Stroke 2015;46:537–44.
[38] Couñago RM, Knapp KM, Nakatani Y, Fleming SB, Corbett M, Wise LM, et al. Structures of Orf virus chemokine binding protein in complex with host chemokines reveal clues to broad binding specificity. Structure 2015;23:1199–213.
[39] Alejo A, Sánchez C, Amu S, Fallon PG, Alcamí A. Addition of a viral immunomodulatory domain to etanercept generates a bifunctional chemokine and TNF inhibitor. J Clin Med 2019;9:25.
[40] Viejo-Borbolla A, Martin AP, Muniz LR, Shang L, Marchesi F, Thirunarayanan N, et al. Attenuation of TNF-driven murine ileitis by intestinal expression of the viral immunomodulator CrmD. Mucosal Immunol 2010;3:633–44.
[41] Xue X, Lu Q, Wei H, Wang D, Chen D, He G, et al. Structural basis of chemokine sequestration by CrmD, a poxvirus-encoded tumor necrosis factor receptor. PLoS Pathog 2011;7:e1002162.
[42] Alejo A, Ruiz-Argüello MB, Ho Y, Smith VP, Saraiva M, Alcami A. A chemokine-binding domain in the tumor

necrosis factor receptor from variola (smallpox) virus. Proc Natl Acad Sci U S A 2006;103:5995–6000.
[43] Millward JM, Holst PJ, Høgh-Petersen M, Thomsen AR, Christensen JP, Owens T. The murine gammaherpesvirus-68 chemokine-binding protein M3 inhibits experimental autoimmune encephalomyelitis. J Neuroimmunol 2010;224:45–50.
[44] Martin AP, Alexander-Brett JM, Canasto-Chibuque C, Garin A, Bromberg JS, Fremont DH, et al. The chemokine binding protein M3 prevents diabetes induced by multiple low doses of streptozotocin. J Immunol 2007;178:4623–31.
[45] Alexander JM, Nelson CA, van Berkel V, Lau EK, Studts JM, Brett TJ, et al. Structural basis of chemokine sequestration by a herpesvirus decoy receptor. Cell 2002;111:343–56.
[46] Alexander-Brett JM, Fremont DH. Dual GPCR and GAG mimicry by the M3 chemokine decoy receptor. J Exp Med 2007;204:3157–72.
[47] Lubman OY, Fremont DH. Parallel evolution of chemokine binding by structurally related herpesvirus decoy receptors. Structure 2016;24:57–69.
[48] Montecucco F, Mach F, Lenglet S, Vonlaufen A, Gomes Quinderé AL, Pelli G, et al. Treatment with Evasin-3 abrogates neutrophil-mediated inflammation in mouse acute pancreatitis. Eur J Clin Invest 2014;44:940–50.
[49] Vieira AT, Fagundes CT, Alessandri AL, Castor MGM, Guabiraba R, Borges VO, et al. Treatment with a novel chemokine-binding protein or eosinophil lineage-ablation protects mice from experimental colitis. Am J Pathol 2009;175:2382–91.
[50] Dias JM, Losberger C, Deruaz M, Power CA, Proudfoot AEI, Shaw JP. Structural basis of chemokine sequestration by a tick chemokine binding protein: the crystal structure of the complex between Evasin-1 and CCL3. PloS One 2009;4:e8514.
[51] Bonvin P, Dunn SM, Rousseau F, Dyer DP, Shaw J, Power CA, et al. Identification of the pharmacophore of the CC chemokine-binding proteins evasin-1 and -4 using phage display. J Biol Chem 2014;289:31846–55.
[52] Franck C, Foster SR, Johansen-Leete J, Chowdhury S, Cielesh M, Bhusal RP, et al. Semisynthesis of an evasin from tick saliva reveals a critical role of tyrosine sulfation for chemokine binding and inhibition. Proc Natl Acad Sci U S A 2020;117:12657–64.
[53] Déruaz M, Frauenschuh A, Alessandri AL, Dias JM, Coelho FM, Russo RC, et al. Ticks produce highly selective chemokine binding proteins with antiinflammatory activity. J Exp Med 2008;205:2019–31.
[54] Lee AW, Deruaz M, Lynch C, Davies G, Singh K, Alenazi Y, et al. A knottin scaffold directs the CXC-chemokine-binding specificity of tick evasins. J Biol Chem 2019;294:11199–212.
[55] Liu L, Dai E, Miller L, Seet B, Lalani A, Macauley C, et al. Viral chemokine-binding proteins inhibit inflammatory responses and aortic allograft transplant vasculopathy in rat models. Transplantation 2004;77:1652–60.
[56] Liu L, Lalani A, Dai E, Seet B, Macauley C, Singh R, et al. The vital anti-inflammatory chemokine-binding protein M-T7 reduces intimal hyperplasia after vascular injury. J Clin Invest 2000;105:1613–21.
[57] Lalani AS, Ness TL, Singh JK, Harrison JK, Seet BT, Kelvin DJ, et al. Functional comparisons among members of the poxvirus T1/35kDa family of soluble CC-chemokine inhibitor glycoproteins. Virology 1998;250:173–84.
[58] Seet BT, Barrett J, Robichaud J, Shilton B, Singh R, McFadden G. Glycosaminoglycan binding properties of the myxoma virus CC-chemokine inhibitor, M-T1. J Biol Chem 2001;276:30504–13.
[59] Lalani AS, Graham K, Mossman K, Rajarathnam K, Clark-Lewis I, Kelvin D, et al. The purified myxoma virus gamma interferon receptor homolog M-T7 interacts with the heparin-binding domains of chemokines. J Virol 1997;71:4356–63.
[60] Burns JM, Dairaghi DJ, Deitz M, Tsang M, Schall TJ. Comprehensive mapping of poxvirus vCCI chemokine-binding protein. Expanded range of ligand interactions and unusual dissociation kinetics. J Biol Chem 2002;277:2785–9.
[61] Kuo NW, Gao YG, Schill MS, Isern N, Dupureur CM, LiWang PJ. Structural insights into the interaction between a potent anti-inflammatory protein, viral CC chemokine inhibitor (vCCI), and the human CC chemokine, eotaxin-1. J Biol Chem 2014;289:6592–603.
[62] Stark LE. Evaluating protein-protein interactions in chemokine-inhibitor complexes through MD simulation. Merced: University of California; 2021.
[63] Seet BT, Singh R, Paavola C, Lau EK, Handel TM, McFadden G. Molecular determinants for CC-chemokine recognition by a poxvirus CC-chemokine inhibitor. Proc Natl Acad Sci USA 2001;98:9008–13.
[64] Beck CG, Studer C, Zuber JF, Demange BJ, Manning U, Urfer R. The viral CC chemokine-binding protein vCCI inhibits monocyte chemoattractant protein-1 activity by masking its CCR2B-binding site. J Biol Chem 2001;276:43270–6.
[65] Ziarek JJ, Heroux MS, Veldkamp CT, Peterson FC, Volkman BF. Sulfotyrosine recognition as marker for druggable sites in the extracellular space. Int J Mol Sci 2011;12:3740–56.
[66] Stark LE, LiWang P, Colvin ME. Determining factors that influence vCCI loop interactions in vCCI-chemokine binding through MD simulation. Biophys J 2020;118:507a.
[67] Stark LE, LiWang PJ, Colvin ME. Evaluating protein - protein interactions in chemokine - inhibitor complexes using MD simulation. Biophys J 2018;114:63a.
[68] LiWang P, Guan W, Stark L, Showalter L, Colvin M. vCCI:Chemokine interactions: experimental biochemistry meets computational prediction. Faseb J 2020;34:1-1.
[69] Nguyen AF, Kuo N-W, Showalter LJ, Ramos R, Dupureur CM, Colvin ME, et al. Biophysical and computational studies of the vCCI:VMIP-II complex. Int J Mol Sci 2017;18:1778.
[70] Saeki H, Tamaki K. Thymus and activation regulated chemokine (TARC)/CCL17 and skin diseases. J Dermatol Sci 2006;43:75–84.
[71] Hansel TT, Tunstall T, Trujillo-Torralbo MB, Shamji B, del-Rosario A, Dhariwal J, et al. A comprehensive evaluation of nasal and bronchial cytokines and chemokines following experimental rhinovirus infection in allergic asthma: increased interferons (IFN-γ and IFN-λ) and type 2 inflammation (IL-5 and IL-13). EBioMedicine 2017;19:128–38.
[72] Roumpeka DD, Wallace RJ, Escalettes F, Fotheringham I, Watson M. A review of bioinformatics tools for bio-prospecting from metagenomic sequence data. Front Genet 2017;8:23.
[73] Zhong S, Macias AT, MacKerell AD Jr. Computational identification of inhibitors of protein-protein interactions. Curr Top Med Chem 2007;7:63–82.
[74] Dror RO, Dirks RM, Grossman JP, Xu H, Shaw DE. Biomolecular simulation: a computational microscope for molecular biology. Annu Rev Biophys 2012;41:429–52.
[75] Frenkel D, Smit B. Understanding molecular simulation. From Algorithms to Applications. 2nd ed. San Diego: Academic Press; 2002.
[76] Dill KA, MacCallum JL. The protein-folding problem, 50 Years on. Science 2012;338:1042–6.
[77] Perez A, Morrone JA, Simmerling C, Dill KA. Advances in free-energy-based simulations of protein folding and ligand binding. Curr Opin Struct Biol 2016;36:25–31.

[78] Shaw DE, Maragakis P, Lindorff-larsen K, Piana S, Shan Y, Wriggers W. Atomic-level characterization of the structural dynamics of proteins. Science 2010;330:341–6.
[79] Kufareva I. Chemokines and their receptors: insights from molecular modeling and crystallography. Curr Opin Pharmacol 2016;30:27–37.
[80] Siebenmorgen T, Zacharias M. Computational prediction of protein–protein binding affinities. Wiley Interdisciplinary Reviews: Computational Molecular Science 2020;10:e1448.
[81] Hansen N, Van Gunsteren WF. Practical aspects of free-energy calculations: a review. J Chem Theor Comput 2014;10:2632–47.
[82] He X, Liu S, Lee TS, Ji B, Man VH, York DM, et al. Fast, accurate, and reliable protocols for routine calculations of protein-ligand binding affinities in drug design projects using AMBER GPU-TI with ff14SB/GAFF. ACS Omega 2020;5:4611–9.
[83] Wang L, Wu Y, Deng Y, Kim B, Pierce L, Krilov G, et al. Accurate and reliable prediction of relative ligand binding potency in prospective drug discovery by way of a modern free-energy calculation protocol and force field. J Am Chem Soc 2015;137:2695–703.
[84] Clark AJ, Gindin T, Zhang B, Wang L, Abel R, Murret CS, et al. Free energy perturbation calculation of relative binding free energy between broadly neutralizing antibodies and the gp120 glycoprotein of HIV-1. J Mol Biol 2017;429:930–47.
[85] Donovan-Maiye RM, Langmead CJ, Zuckerman DM. Systematic testing of belief-propagation estimates for absolute free energies in atomistic peptides and proteins. J Chem Theor Comput 2018;14:426–43.
[86] Geng C, Xue LC, Roel-Touris J, Bonvin AMJJ. Finding the ΔΔG spot: are predictors of binding affinity changes upon mutations in protein–protein interactions ready for it? Wiley Interdisciplinary Reviews: Computational Molecular Science 2019;9:1–14.
[87] Lodi PJ, Garrett DS, Kuszewski J, Tsang MLS, Weatherbee JA, Leonard WJ, et al. High-resolution solution structure of the β chemokine hMIP-1β by multidimensional NMR. Science 1994;263:1762–7.
[88] Kim S, Jao S, Laurence JS, LiWang PJ. Structural comparison of monomeric variants of the chemokine MIP-1β having differing ability to bind the receptor CCR5. Biochemistry 2001;40:10782–91.
[89] Pettersen EF, Goddard TD, Huang CC, Couch GS, Greenblatt DM, Meng EC, et al. UCSF Chimera–a visualization system for exploratory research and analysis. J Comput Chem 2004;25:1605–12.